

11.5 Load Transfer Mechanism

The load transfer mechanism from a pile to the soil is complicated. To understand it, consider a pile of length L , as shown in Figure 11.9a. The load on the pile is gradually increased from zero to $Q_{(z=0)}$ at the ground surface. Part of this load will be resisted by the side friction developed along the shaft, Q_1 , and part by the soil below the tip of

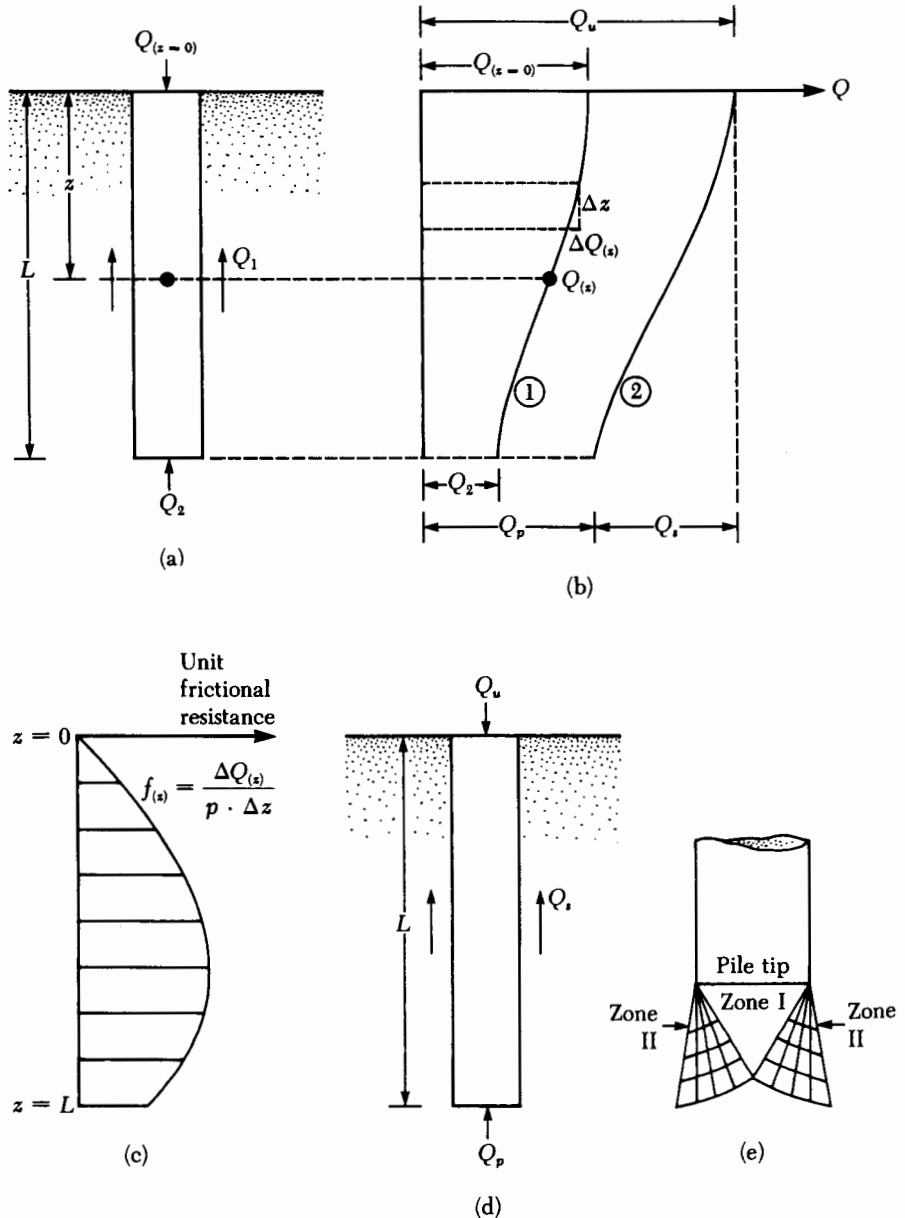


Figure 11.9 Load transfer mechanism for piles

the pile, Q_2 . Now, how are Q_1 and Q_2 related to the total load? If measurements are made to obtain the load carried by the pile shaft, $Q_{(z)}$, at any depth z , the nature of the variation found will be like that shown in curve 1 of Figure 11.9b. The *frictional resistance per unit area* at any depth z may be determined as

$$f_{(z)} = \frac{\Delta Q_{(z)}}{(p)(\Delta z)} \quad (11.8)$$

where p = perimeter of the cross section of the pile

Figure 11.9c shows the variation of $f_{(z)}$ with depth.

If the load Q at the ground surface is gradually increased, maximum frictional resistance along the pile shaft will be fully mobilized when the relative displacement between the soil and the pile is about 5–10 mm (0.2–0.3 in.), irrespective of the pile size and length L . However, the maximum point resistance $Q_2 = Q_p$ will not be mobilized until the tip of the pile has moved about 10–25% of the pile width (or diameter). (The lower limit applies to driven piles and the upper limit to bored piles). At ultimate load (Figure 11.9d and curve 2 in Figure 11.9b), $Q_{(z=0)} = Q_u$. Thus,

$$Q_1 = Q_s$$

and

$$Q_2 = Q_p$$

The preceding explanation indicates that Q_s (or the unit skin friction, f , along the pile shaft) is developed at a *much smaller pile displacement compared with the point resistance, Q_p* .

At ultimate load, the failure surface in the soil at the pile tip (a bearing capacity failure caused by Q_p) is like that shown in Figure 11.9e. Note that pile foundations are deep foundations and that the soil fails mostly in a *punching mode*, as illustrated previously in Figures 3.1c and 3.3. That is, a *triangular zone*, I, is developed at the pile tip, which is pushed downward without producing any other visible slip surface. In dense sands and stiff clayey soils, a *radial shear zone*, II, may partially develop. Hence, the load displacement curves of piles will resemble those shown in Figure 3.1c.

11.6

Equations for Estimating Pile Capacity

The ultimate load-carrying capacity Q_u of a pile is given by the equation

$$Q_u = Q_p + Q_s \quad (11.9)$$

where Q_p = load-carrying capacity of the pile point

Q_s = frictional resistance (skin friction) derived from the soil–pile interface (see Figure 11.10)

Numerous published studies cover the determination of the values of Q_p and Q_s . Excellent reviews of many of these investigations have been provided by Vesic (1977), Meyerhof (1976), and Coyle and Castello (1981). These studies afford an insight into the problem of determining the ultimate pile capacity.

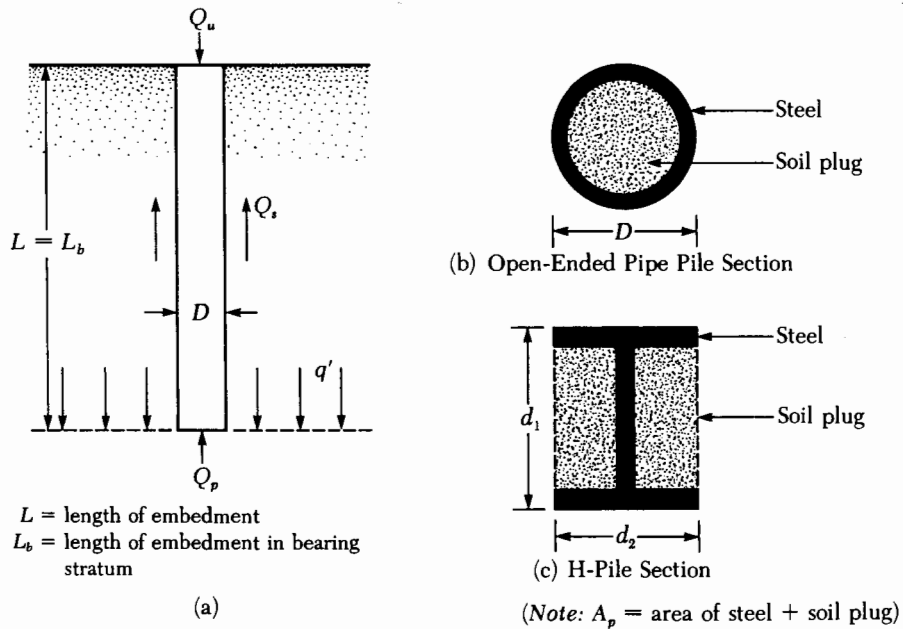


Figure 11.10 Ultimate load-carrying capacity of pile

Point Bearing Capacity, Q_p

The ultimate bearing capacity of shallow foundations was discussed in Chapter 3. According to Terzaghi's equations,

$$q_u = 1.3c'N_c + qN_q + 0.4\gamma BN_\gamma \quad (\text{for shallow square foundations})$$

and

$$q_u = 1.3c'N_c + qN_q + 0.3\gamma BN_\gamma \quad (\text{for shallow circular foundations})$$

Similarly, the general bearing capacity equation for shallow foundations was given in Chapter 3 (for vertical loading) as

$$q_u = c'N_cF_{cs}F_{cd} + qN_qF_{qs}F_{qd} + \frac{1}{2}\gamma BN_\gamma F_{\gamma s}F_{\gamma d}$$

Hence, in general, the ultimate load-bearing capacity may be expressed as

$$q_u = c'N_c^* + qN_q^* + \gamma BN_\gamma^* \quad (11.10)$$

where N_c^* , N_q^* , and N_γ^* are the bearing capacity factors that include the necessary shape and depth factors

Pile foundations are deep. However, the ultimate resistance per unit area developed at the pile tip, q_p , may be expressed by an equation similar in form to Eq. (11.10), although the values of N_c^* , N_q^* , and N_γ^* will change. The notation used in this chapter for the width of a pile is D . Hence, substituting D for B in Eq. (11.10) gives

$$q_u = q_p = c'N_c^* + qN_q^* + \gamma DN_\gamma^* \quad (11.11)$$

Because the width D of a pile is relatively small, the term γDN_γ^* may be dropped from the right side of the preceding equation without introducing a serious error; thus, we have

$$q_p = c'N_c^* + q'N_q^* \quad (11.12)$$

Note that the term q has been replaced by q' in Eq. (11.12), to signify effective vertical stress. Thus, the point bearing of piles is

$$Q_p = A_p q_p = A_p (c'N_c^* + q'N_q^*) \quad (11.13)$$

where A_p = area of pile tip
 c' = cohesion of the soil supporting the pile tip
 q_p = unit point resistance
 q' = effective vertical stress at the level of the pile tip
 N_c^*, N_q^* = the bearing capacity factors

Frictional Resistance, Q_s

The frictional, or skin, resistance of a pile may be written as

$$Q_s = \sum p \Delta L f \quad (11.14)$$

where p = perimeter of the pile section
 ΔL = incremental pile length over which p and f are taken to be constant
 f = unit friction resistance at any depth z

The various methods for estimating Q_p and Q_s are discussed in the next several sections. It needs to be reemphasized that, in the field, for full mobilization of the point resistance (Q_p), the pile tip must go through a displacement of 10 to 25% of the pile width (or diameter).

11.7

Meyerhof's Method for Estimating Q_p

Sand

The point bearing capacity, q_p , of a pile in sand generally increases with the depth of embedment in the bearing stratum and reaches a maximum value at an embedment ratio of $L_b/D = (L_b/D)_{cr}$. Note that in a homogeneous soil L_b is equal to the actual embedment length of the pile, L . (See Figure 11.10a.) However, where a pile has penetrated into a bearing stratum, $L_b < L$. (See Figure 11.6b.) Beyond the critical embedment ratio, $(L_b/D)_{cr}$, the value of q_p remains constant ($q_p = q_{li}$). That is, as shown in Figure 11.11 for the case of a homogeneous soil, $L = L_b$.

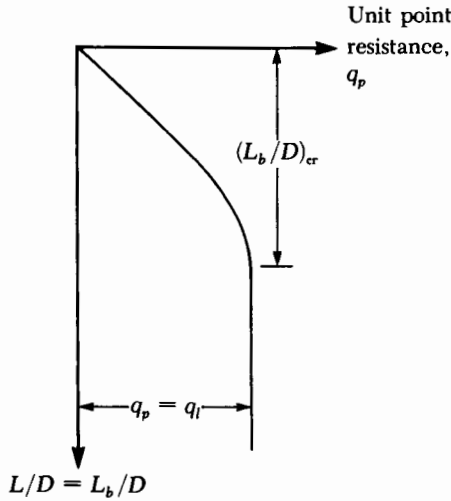


Figure 11.11 Nature of variation of unit point resistance in a homogeneous sand

For piles in sand, $c' = 0$, and Eq. (11.13) simplifies to

$$Q_p = A_p q_p = A_p q' N_q^* \tag{11.15}$$

The variation of N_q^* with soil friction angle ϕ' is shown in Figure 11.12. However, Q_p should not exceed the limiting value $A_p q_l$; that is,

$$Q_p = A_p q' N_q^* \leq A_p q_l \tag{11.16}$$

The limiting point resistance is

$$q_l = 0.5 p_a N_q^* \tan \phi' \tag{11.17}$$

where p_a = atmospheric pressure (=100 kN/m² or 2000 lb/ft²)
 ϕ' = effective soil friction angle of the bearing stratum

On the basis of field observations, Meyerhof (1976) also suggested that the ultimate point resistance q_p in a homogeneous granular soil ($L = L_b$) may be obtained from standard penetration numbers as

$$q_l = 0.4 p_a (N_1)_{60} \frac{L}{D} \leq 4 p_a (N_1)_{60} \tag{11.18}$$

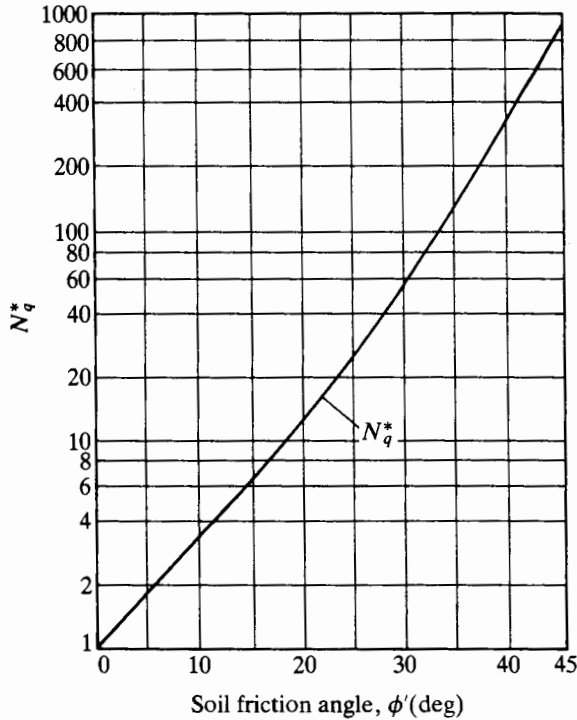


Figure 11.12 Variation of the maximum values of N_q^* with soil friction angle ϕ' (after Meyerhof, 1976)

where $(N_1)_{60}$ = the average corrected value of the standard penetration number near the pile point (about $10D$ above and $4D$ below the pile point)
 p_a = atmospheric pressure ($\approx 100 \text{ kN/m}^2$ or 2000 lb/ft^2)

Clay ($\phi = 0$)

For piles in *saturated clays* under undrained conditions ($\phi = 0$),

$$Q_p = N_c^* c_u A_p = 9c_u A_p \quad (11.19)$$

where c_u = undrained cohesion of the soil below the tip of the pile

11.8

Vesic's Method for Estimating Q_p

Vesic (1977) proposed a method for estimating the pile point bearing capacity based on the theory of *expansion of cavities*. According to this theory, on the basis of effective stress parameters, we may write

$$Q_p = A_p q_p = A_p (c' N_c^* + \bar{\sigma}'_o N_\sigma^*) \quad (11.20)$$

where $\bar{\sigma}_o =$ mean effective normal ground stress at the level of the pile point

$$= \left(\frac{1 + 2K_o}{3} \right) q'$$
 (11.21)

$K_o =$ earth pressure coefficient at rest $= 1 - \sin \phi'$ (11.22)
 $N_c^*, N_\sigma^* =$ bearing capacity factors

Note that Eq. (11.20) is a modification of Eq. (11.13) with

$$N_\sigma^* = \frac{3N_q^*}{(1 + 2K_o)}$$
 (11.23)

Note also that N_c^* in Eq. (11.20) may be expressed as

$$N_c^* = (N_q^* - 1) \cot \phi'$$
 (11.24)

According to Vesic's theory,

$$N_\sigma^* = f(I_{rr})$$
 (11.25)

where $I_{rr} =$ reduced rigidity index for the soil

However,
$$I_{rr} = \frac{I_r}{1 + I_r \Delta}$$
 (11.26)

where $I_r =$ rigidity index $= \frac{E_s}{2(1 + \mu_s)(c' + q' \tan \phi')} = \frac{G_s}{c' + q' \tan \phi'}$ (11.27)

$E_s =$ modulus of elasticity of soil

$\mu_s =$ Poisson's ratio of soil

$G_s =$ shear modulus of soil

$\Delta =$ average volumatic strain in the plastic zone below the pile point

When the volume does not change (e.g., for dense sand or saturated clay), $\Delta = 0$, so

$$I_r = I_{rr}$$
 (11.28)

Table 11.4 gives the values of N_c^* and N_σ^* for various values of the soil friction angle ϕ' and I_{rr} . For $\phi = 0$ (an undrained condition),

$$N_c^* = \frac{4}{3}(\ln I_{rr} + 1) + \frac{\pi}{2} + 1$$
 (11.29)

The values of I_r can be estimated from laboratory consolidation and triaxial tests corresponding to the proper stress levels. However, for preliminary use, the following values are recommended:

Type of soil	I_r
Sand	70–150
Silts and clays (drained condition)	50–100
Clays (undrained condition)	100–200

Table 11.4 Bearing Capacity Factors N_c^* and N_q^* Based on the Theory of Expansion of Cavities

ϕ'	I_r									
	10	20	40	60	80	100	200	300	400	500
0	6.97	7.90	8.82	9.36	9.75	10.04	10.97	11.51	11.89	12.19
1	1.00	1.00	1.00	1.00	1.00	1.00	1.00	1.00	1.00	1.00
2	7.34	8.37	9.42	10.04	10.49	10.83	11.92	12.57	13.03	13.39
3	1.13	1.15	1.16	1.18	1.18	1.19	1.21	1.22	1.23	1.23
4	7.72	8.87	10.06	10.77	11.28	11.69	12.96	13.73	14.28	14.71
5	1.27	1.31	1.35	1.38	1.39	1.41	1.45	1.48	1.50	1.51
6	8.12	9.40	10.74	11.55	12.14	12.61	14.10	15.00	15.66	16.18
7	1.43	1.49	1.56	1.61	1.64	1.66	1.74	1.79	1.82	1.85
8	8.54	9.96	11.47	12.40	13.07	13.61	15.34	16.40	17.18	17.80
9	1.60	1.70	1.80	1.87	1.91	1.95	2.07	2.15	2.20	2.24
10	8.99	10.56	12.25	13.30	14.07	14.69	16.69	17.94	18.86	19.59
11	1.79	1.92	2.07	2.16	2.23	2.28	2.46	2.57	2.65	2.71
12	9.45	11.19	13.08	14.26	15.14	15.85	18.17	19.62	20.70	21.56
13	1.99	2.18	2.37	2.50	2.59	2.67	2.91	3.06	3.18	3.27
14	9.94	11.85	13.96	15.30	16.30	17.10	19.77	21.46	22.71	23.73
15	2.22	2.46	2.71	2.88	3.00	3.10	3.43	3.63	3.79	3.91
16	10.45	12.55	14.90	16.41	17.54	18.45	21.51	23.46	24.93	26.11
17	2.47	2.76	3.09	3.31	3.46	3.59	4.02	4.30	4.50	4.67
18	10.99	13.29	15.91	17.59	18.87	19.90	23.39	25.64	27.35	28.73
19	2.74	3.11	3.52	3.79	3.99	4.15	4.70	5.06	5.33	5.55
20	11.55	14.08	16.97	18.86	20.29	21.46	25.43	28.02	29.99	31.59
21	3.04	3.48	3.99	4.32	4.58	4.78	5.48	5.94	6.29	6.57
22	12.14	14.90	18.10	20.20	21.81	23.13	27.64	30.61	32.87	34.73
23	3.36	3.90	4.52	4.93	5.24	5.50	6.37	6.95	7.39	7.75
24	12.76	15.77	19.30	21.64	23.44	24.92	30.03	33.41	36.02	38.16
25	3.71	4.35	5.10	5.60	5.98	6.30	7.38	8.10	8.66	9.11
26	13.41	16.69	20.57	23.17	25.18	26.84	32.60	36.46	39.44	41.89
27	4.09	4.85	5.75	6.35	6.81	7.20	8.53	9.42	10.10	10.67
28	14.08	17.65	21.92	24.80	27.04	28.89	35.38	39.75	43.15	45.96
29	4.51	5.40	6.47	7.18	7.74	8.20	9.82	10.91	11.76	12.46
30	14.79	18.66	23.35	26.53	29.02	31.08	38.37	43.32	47.18	50.39
31	4.96	6.00	7.26	8.11	8.78	9.33	11.28	12.61	13.64	14.50
32	15.53	19.73	24.86	28.37	31.13	33.43	41.58	47.17	51.55	55.20
33	5.45	6.66	8.13	9.14	9.93	10.58	12.92	14.53	15.78	16.83

Table 11.4 (Continued)

ϕ'	I_r									
	10	20	40	60	80	100	200	300	400	500
17	16.30	20.85	26.46	30.33	33.37	35.92	45.04	51.32	56.27	60.42
18	5.98	7.37	9.09	10.27	11.20	11.98	14.77	16.99	18.20	19.47
19	17.11	22.03	28.15	32.40	35.76	38.59	48.74	55.80	61.38	66.07
20	6.56	8.16	10.15	11.53	12.62	13.54	16.84	19.13	20.94	22.47
21	17.95	23.26	29.93	34.59	38.30	41.42	52.71	60.61	66.89	72.18
22	7.18	9.01	11.31	12.91	14.19	15.26	19.15	21.87	24.03	25.85
23	18.83	24.56	31.81	36.92	40.99	44.43	56.97	65.79	72.82	78.78
24	7.85	9.94	12.58	14.44	15.92	17.17	21.73	24.94	27.51	29.67
25	19.75	25.92	33.80	39.38	43.85	47.64	61.51	71.34	79.22	85.90
26	8.58	10.95	13.97	16.12	17.83	19.29	24.61	28.39	31.41	33.97
27	20.71	27.35	35.89	41.98	46.88	51.04	66.37	77.30	86.09	93.57
28	9.37	12.05	15.50	17.96	19.94	21.62	27.82	32.23	35.78	38.81
29	21.71	28.84	38.09	44.73	50.08	54.66	71.56	83.68	93.47	101.83
30	10.21	13.24	17.17	19.99	22.26	24.20	31.37	36.52	40.68	44.22
31	22.75	30.41	40.41	47.63	53.48	58.49	77.09	90.51	101.39	110.70
32	11.13	14.54	18.99	22.21	24.81	27.04	35.32	41.30	46.14	50.29
33	23.84	32.05	42.85	50.69	57.07	62.54	82.98	97.81	109.88	120.23
34	12.12	15.95	20.98	24.64	27.61	30.16	39.70	46.61	52.24	57.06
35	24.98	33.77	45.42	53.93	60.87	66.84	89.25	105.61	118.96	130.44
36	13.18	17.47	23.15	27.30	30.69	33.60	44.53	52.51	59.02	64.62
37	26.16	35.57	48.13	57.34	64.88	71.39	95.02	113.92	128.67	141.39
38	14.33	19.12	25.52	30.21	34.06	37.37	49.88	59.05	66.56	73.04
39	27.40	37.45	50.96	60.93	69.12	76.20	103.01	122.79	139.04	153.10
40	15.57	20.91	28.10	33.40	37.75	41.51	55.77	66.29	74.93	82.40
41	28.69	39.42	53.95	64.71	73.58	81.28	110.54	132.23	150.11	165.61
42	16.90	22.85	30.90	36.87	41.79	46.05	62.27	74.30	84.21	92.80
43	30.03	41.49	57.08	68.69	78.30	86.64	118.53	142.27	161.91	178.98
44	18.24	24.95	33.95	40.66	46.21	51.02	69.43	83.14	94.48	104.33
45	31.43	43.64	60.37	72.88	83.27	92.31	126.99	152.95	174.49	193.23
46	19.88	27.22	37.27	44.79	51.03	56.46	77.31	92.90	105.84	117.11
47	32.89	45.90	63.82	77.29	88.50	98.28	135.96	164.29	187.87	208.43
48	21.55	29.68	40.88	49.30	56.30	62.41	85.96	103.66	118.39	131.24
49	34.41	48.26	67.44	81.92	94.01	104.58	145.46	176.33	202.09	224.62
50	23.34	32.34	44.80	54.20	62.05	68.92	95.46	115.51	132.24	146.87
51	35.99	50.72	71.24	86.80	99.82	111.22	155.51	189.11	217.21	241.84
52	25.28	35.21	49.05	59.54	68.33	76.02	105.90	128.55	147.51	164.12

Table 11.4 (Continued)

ϕ'	I_r									
	10	20	40	60	80	100	200	300	400	500
35	37.65	53.30	75.22	91.91	105.92	118.22	166.14	202.64	233.27	260.15
36	27.36	38.32	53.67	65.36	75.17	83.78	117.33	142.89	164.33	183.16
	39.37	55.99	79.39	97.29	112.34	125.59	177.38	216.98	250.30	279.60
37	29.60	41.68	58.68	71.69	82.62	92.24	129.87	158.65	182.85	204.14
	41.17	58.81	83.77	102.94	119.10	133.34	189.25	232.17	268.36	300.26
38	32.02	45.31	64.13	78.57	90.75	101.48	143.61	175.95	203.23	227.26
	43.04	61.75	88.36	108.86	126.20	141.50	201.78	248.23	287.50	322.17
39	34.63	49.24	70.03	86.05	99.60	111.56	158.65	194.94	225.62	252.71
	44.99	64.83	93.17	115.09	133.66	150.09	215.01	265.23	307.78	345.41
40	37.44	53.50	76.45	94.20	109.24	122.54	175.11	215.78	250.23	280.71
	47.03	68.04	98.21	121.62	141.51	159.13	228.97	283.19	329.24	370.04
41	40.47	58.10	83.40	103.05	119.74	134.52	193.13	238.62	277.26	311.50
	49.16	71.41	103.49	128.48	149.75	168.63	243.69	302.17	351.95	396.12
42	43.74	63.07	90.96	112.68	131.18	147.59	212.84	263.67	306.94	345.34
	51.38	74.92	109.02	135.68	158.41	178.62	259.22	322.22	375.97	423.74
43	47.27	68.46	99.16	123.16	143.64	161.83	234.40	291.13	339.52	382.53
	53.70	78.60	114.82	143.23	167.51	189.13	275.59	343.40	401.36	452.96
44	51.08	74.30	108.08	134.56	157.21	177.36	257.99	321.22	375.28	423.39
	56.13	82.45	120.91	151.16	177.07	200.17	292.85	365.75	428.21	483.88
45	55.20	80.62	117.76	146.97	172.00	194.31	283.80	354.20	414.51	468.28
	58.66	86.48	127.28	159.48	187.12	211.79	311.04	389.35	456.57	516.58
46	59.66	87.48	128.28	160.48	188.12	212.79	312.03	390.35	457.57	517.58
	61.30	90.70	133.97	168.22	197.67	224.00	330.20	414.26	486.54	551.16
47	64.48	94.92	139.73	175.20	205.70	232.96	342.94	429.98	504.82	571.74
	64.07	95.12	140.99	177.40	208.77	236.85	350.41	440.54	518.20	587.72
48	69.71	103.00	152.19	191.24	224.88	254.99	376.77	473.42	556.70	631.25
	66.97	99.75	148.35	187.04	220.43	250.36	371.70	468.28	551.64	626.36
49	75.38	111.78	165.76	208.73	245.81	279.06	413.82	521.08	613.65	696.64
	70.01	104.60	156.09	197.17	232.70	264.58	394.15	497.56	586.96	667.21
50	81.54	121.33	180.56	227.82	268.69	305.37	454.42	573.38	676.22	768.53
	73.19	109.70	164.21	207.83	245.60	279.55	417.82	528.46	624.28	710.39
	88.23	131.73	196.70	248.68	293.70	334.15	498.94	630.80	744.99	847.61

From "Design of Pile Foundations," by A. S. Vesic, in *NCHRP Synthesis of Highway Practice 42*, Transportation Research Board, 1977. Reprinted by permission.

Note: Upper number N_c^* , lower number N_c^* .

On the basis of cone penetration tests in the field, Baldi et al. (1981) gave the following correlations for I_r :

$$I_r = \frac{300}{F_r(\%)} \quad (\text{for mechanical cone penetration}) \quad (11.30a)$$

and

$$I_r = \frac{170}{F_r(\%)} \quad (\text{for electric cone penetration}) \quad (11.30b)$$

For the definition of F_r , see Eq. (2.37).

11.9 Janbu's Method for Estimating Q_p

Janbu (1976) proposed calculating Q_p as follows:

$$Q_p = A_p(c'N_c^* + q'N_q^*) \quad (11.31)$$

Note that Eq. (11.31) has the same form as Eq. (11.13). The bearing capacity factors N_c^* and N_q^* are calculated by assuming a failure surface in soil at the pile tip similar to that shown in Figure 11.13. The bearing capacity relationships are then

$$N_q^* = (\tan \phi' + \sqrt{1 + \tan^2 \phi'})^2 (e^{2\eta' \tan \phi'}) \quad (11.32a)$$

(the angle η' is defined in the figure) and

$$N_c^* = (N_q^* - 1) \cot \phi' \quad (11.32b)$$

↑
from Eq. (11.32a)

The angle η' varies from 60° for soft clays to about 105° for dense sandy soils. It is recommended that, for practical use,

$$60^\circ \leq \eta' \leq 90^\circ$$

Table 11.5 gives the variation of N_c^* and N_q^* for $\eta' = 60^\circ, 75^\circ$, and 90° .

11.10 Coyle and Castello's Method for Estimating Q_p in Sand

Coyle and Castello (1981) analyzed 24 large-scale field load tests of driven piles in sand. On the basis of the test results, they suggested that, in sand,

$$Q_p = q'N_q^*A_p \quad (11.33)$$

where q' = effective vertical stress at the pile tip
 N_q^* = bearing capacity factor

Figure 11.14 shows the variation of N_q^* with L/D and the soil friction angle ϕ' .

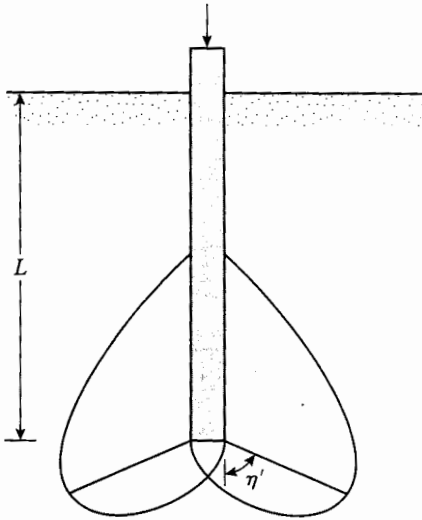


Figure 11.13 Failure surface at the pile tip

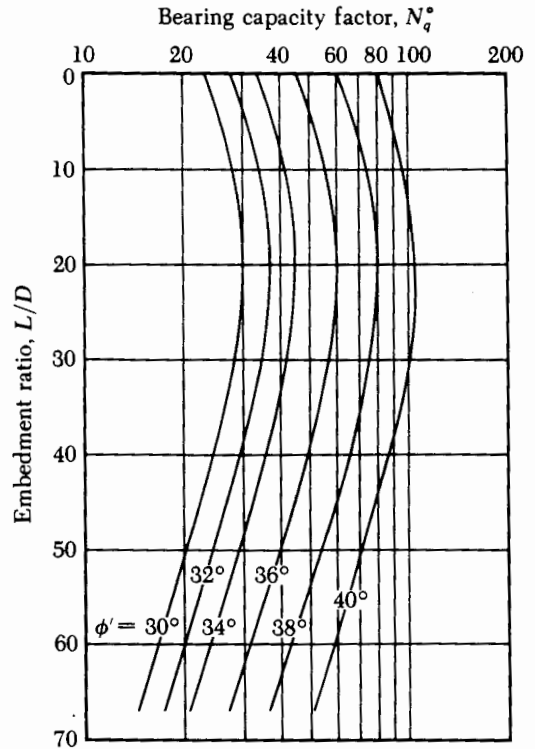


Figure 11.14 Variation of N_q^* with L/D (redrawn after Coyle and Castello, 1981)

Table 11.5 Janbu's Bearing Capacity Factors

ϕ'°	$\eta' = 60^\circ$		$\eta' = 75^\circ$		$\eta' = 90^\circ$	
	N_c^*	N_q^*	N_c^*	N_q^*	N_c^*	N_q^*
0	5.74	1.0	5.74	1.0	5.74	1.0
10	5.95	2.05	7.11	2.25	8.34	2.47
20	9.26	4.37	11.78	5.29	14.83	6.40
30	19.43	10.05	21.82	13.60	30.14	18.40
40	30.58	26.66	48.11	41.37	75.31	64.20
45	46.32	47.32	78.90	79.90	133.87	134.87

11.11

Other Correlations for Calculating Q_p with SPT and CPT Results

There are several correlations in the literature for calculating Q_p on the basis of standard penetration test and cone penetration test results conducted in the field. We summarize some of these correlations in this section. Table 11.6 gives the correlation

Table 11.6 Correlations with Standard Penetration Resistance

Reference	Relationship	Applicability
Briaud et al. (1985)	$q_p = 19.7 p_a (N_{60})^{0.36}$	Sand
Shioi and Fukui (1982)	$q_p = 3 p_a$	Cast in place, sand
	$q_p = 0.1 p_a N_{60}$	Bored pile, sand
	$q_p = 0.15 p_a N_{60}$	Bored pile, gravelly sand
	$q_p = 0.3 p_a N_{60}$	Driven piles, all soils

of q_p with the standard penetration number N_{60} . It is important to note that the N_{60} value is the average condition near the pile tip (i.e., $4D$ below and $10D$ above the pile tip).

There are two major methods for estimating the magnitude of q_p using the cone penetration resistance q_c :

1. The LCPC method, developed by Laboratoire Central des Ponts at Chaussées (Bustamante and Gianceselli, 1982); and
2. The Dutch method (DeRuiter and Beringer, 1979).

LCPC Method

According to the LCPC method,

$$q_p = q_{c(\text{eq})} k_b \quad (11.34)$$

where $q_{c(\text{eq})}$ = equivalent average cone resistance
 k_b = empirical bearing capacity factor

The magnitude of $q_{c(\text{eq})}$ is calculated in the following manner:

1. Consider the cone tip resistance q_c within a range of $1.5D$ below the pile tip to $1.5D$ above the pile tip, as shown in Figure 11.15.
2. Calculate the average value of q_c [$q_{c(\text{av})}$] within the zone shown in Figure 11.15.
3. Eliminate the q_c values that are higher than $1.3q_{c(\text{av})}$ and the q_c values that are lower than $0.7q_{c(\text{av})}$.
4. Calculate $q_{c(\text{eq})}$ by averaging the remaining q_c values.

Briaud and Miran (1991) suggested that

$$k_b = 0.6 \text{ (for clays and silts)}$$

and

$$k_b = 0.375 \text{ (for sands and gravels)}$$

Dutch Method

According to the Dutch method, one considers the variation of q_c in the range of $4D$ below the pile tip to $8D$ above the pile tip, as shown in Figure 11.16. Then one conducts the following operations:

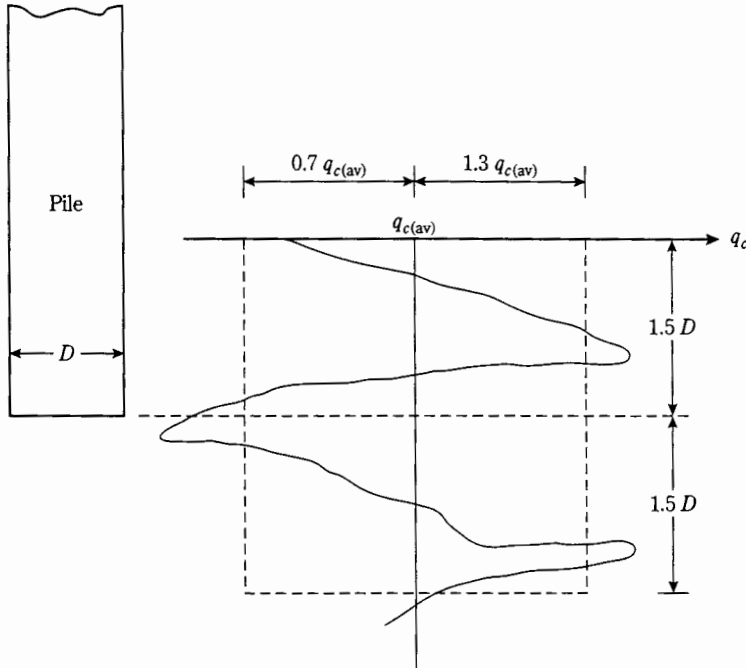


Figure 11.15 LCPC method

1. Average the q_c values over a distance yD below the pile tip. This is path $a-b-c$. Sum q_c values along the downward path $a-b$ (i.e., the actual path a) and the upward path $b-c$ (i.e., the minimum path). Determine the minimum value q_{c1} = average value of q_c for $0.7 < y < 4$.
2. Average the q_c values (q_{c2}) between the pile tip and $8D$ above the pile tip along the path $c-d-e-f-g$, using the minimum path and ignoring minor peak depressions.
3. Calculate

$$q_p = \frac{(q_{c1} + q_{c2})}{2} k'_b \leq 150 p_a \quad (11.35)$$

where p_a = atmospheric pressure ($\approx 100 \text{ kN/m}^2$, or 2000 lb/ft^2)

DeRuiter and Beringen (1979) recommended the following values for k'_b for sand:

- 1.0 for OCR (overconsolidation ratio) = 1
- 0.67 for OCR = 2 to 4

Nottingham and Schmertmann (1975) and Schmertmann (1978) recommended the following relationship for q_p in clay:

$$q_p = R_1 R_2 \frac{(q_{c1} + q_{c2})}{2} k'_b \leq 150 p_a \quad (11.36)$$

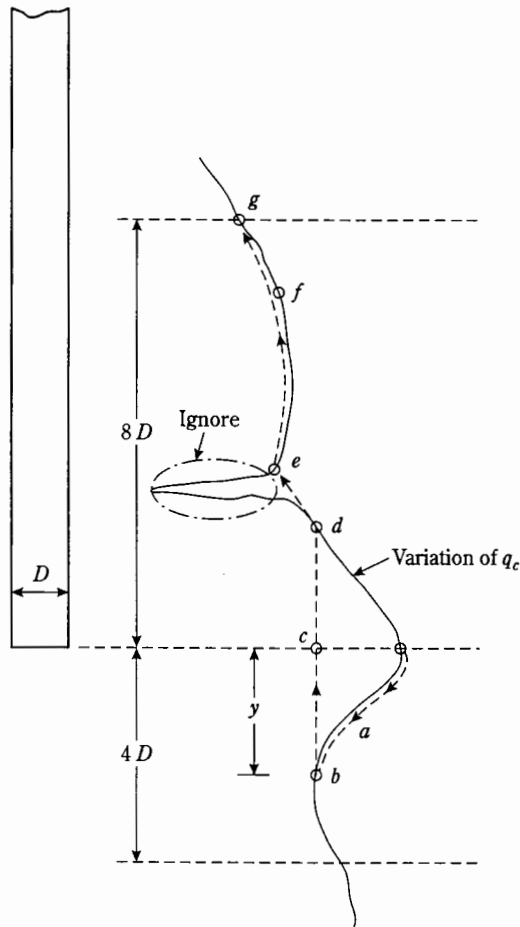


Figure 11.16 Dutch method

In this equation, R_1 = reduction factor, which is a function of the undrained shear strength c_u

$R_2 = 1$ for electric cone penetrometer; = 0.6 for mechanical cone penetrometer

The interpolated values of R_1 with c_u provided by Schmertmann (1978) are as follows:

$\frac{c_u}{p_a}$	R_1
≥ 0.5	1
0.75	0.64
1.0	0.53
1.25	0.42
1.5	0.36
1.75	0.33
2.0	0.30

11.12 Frictional Resistance (Q_s) in Sand

According to Eq. (11.14), the frictional resistance

$$Q_s = \sum p \Delta L f$$

The unit frictional resistance, f , is hard to estimate. In making an estimation of f , several important factors must be kept in mind:

1. The nature of the pile installation. For driven piles in sand, the vibration caused during pile driving helps densify the soil around the pile. Figure 11.17 shows the contours of the soil friction angle ϕ' around a driven pile (Meyerhof, 1961). Note that, in this case, the original effective soil friction angle of the sand was 32° . The zone of sand densification is about 2.5 times the pile diameter, in the sand surrounding the pile.
2. It has been observed that the nature of variation of f in the field is approximately as shown in Figure 11.18. The unit skin friction increases with depth more or less

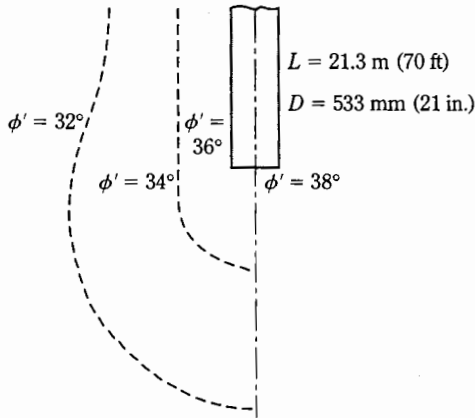


Figure 11.17 Compaction of sand near driven piles (after Meyerhof, 1961)

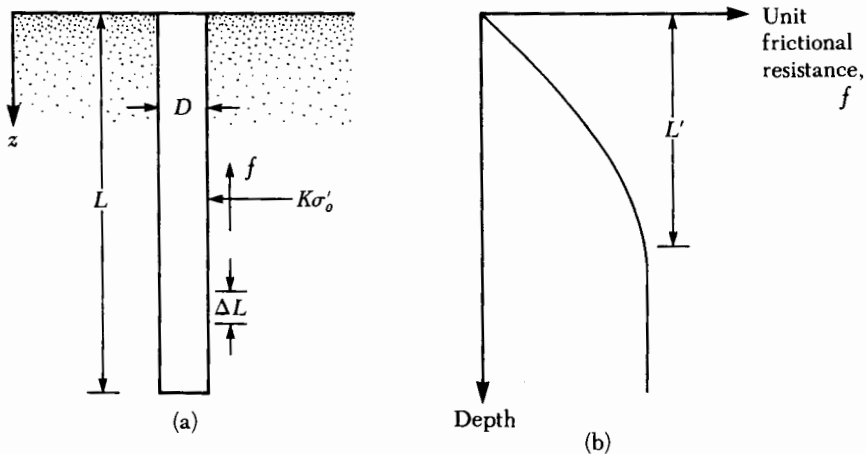


Figure 11.18 Unit frictional resistance for piles in sand

linearly to a depth of L' and remains constant thereafter. The magnitude of the critical depth L' may be 15 to 20 pile diameters. A conservative estimate would be

$$L' \approx 15D \quad (11.37)$$

3. At similar depths, the unit skin friction in loose sand is higher for a high-displacement pile, compared with a low-displacement pile.
4. At similar depths, bored, or jetted, piles will have a lower unit skin friction, compared with driven piles.

Taking into account the preceding factors, we can give the following approximate relationship for f (see Figure 11.18):

For $z = 0$ to L' ,

$$f = K\sigma'_o \tan \delta \quad (11.38)$$

and for $z = L'$ to L ,

$$f = f_{z=L'} \quad (11.39)$$

In these equations, K = effective earth coefficient
 σ'_o = effective vertical stress at the depth under consideration
 δ = soil-pile friction angle

In reality, the magnitude of K varies with depth; it is approximately equal to the Rankine passive earth pressure coefficient, K_p , at the top of the pile and may be less than the at-rest pressure coefficient, K_o , at a greater depth. Based on presently available results, the following average values of K are recommended for use in Eq. (11.38):

Pile type	K
Bored or jetted	$\approx K_o = 1 - \sin \phi'$
Low-displacement driven	$\approx K_o = 1 - \sin \phi'$ to $1.4K_o = 1.4(1 - \sin \phi')$
High-displacement driven	$\approx K_o = 1 - \sin \phi'$ to $1.8K_o = 1.8(1 - \sin \phi')$

The values of δ from various investigations appear to be in the range from $0.5\phi'$ to $0.8\phi'$. Judgment must be used in choosing the value of δ . For high-displacement driven piles, Bhusan (1982) recommended

$$K \tan \delta = 0.18 + 0.0065D_r \quad (11.40)$$

and

$$K = 0.5 + 0.008D_r \quad (11.41)$$

where D_r = relative density (%)

Coyle and Castello (1981), in conjunction with the material presented in Section 11.10, proposed that

$$Q_s = f_{av}pL = (K\bar{\sigma}'_o \tan \delta)pL \quad (11.42)$$

where $\bar{\sigma}'_o$ = average effective overburden pressure
 δ = soil-pile friction angle = $0.8\phi'$

The lateral earth pressure coefficient K , which was determined from field observations, is shown in Figure 11.19. Thus, if that figure is used,

$$Q_s = K\bar{\sigma}'_o \tan(0.8\phi') pL \tag{11.43}$$

Correlation with Standard Penetration Test Results

Meyerhof (1976) indicated that the average unit frictional resistance, f_{av} , for high-displacement driven piles may be obtained from average corrected standard penetration resistance values as

$$f_{av} = 0.02 p_a (\bar{N}_1)_{60} \tag{11.44}$$

where $(\bar{N}_1)_{60}$ = average corrected value of standard penetration resistance
 p_a = atmospheric pressure ($\approx 100 \text{ kN/m}^2$ or 2000 lb/ft^2)

For low-displacement driven piles

$$f_{av} = 0.01 p_a (\bar{N}_1)_{60} \tag{11.45}$$

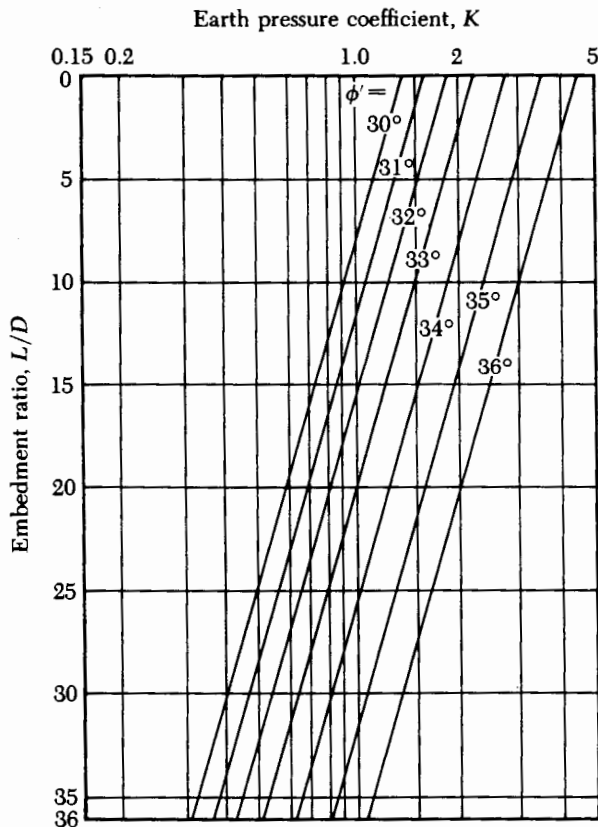


Figure 11.19 Variation of K with L/D (redrawn after Coyle and Castello, 1981)

Thus,

$$Q_s = pL f_{av} \quad (11.46)$$

Briaud et al. (1985) proposed another correlation for unit skin friction with the standard penetration resistance, in the form

$$f = 0.224 p_a (N_{60})^{0.29} \quad (11.47)$$

Hence,

$$Q_s = \Sigma p(\Delta L) f = \Sigma 0.224 p p_a(\Delta L) (N_{60})^{0.29} \quad (11.48)$$

In a fairly homogeneous soil, we can estimate the average value of N_{60} . In that case,

$$Q_s = pL f_{av}$$

$$\text{where } f_{av} = 0.224 p_a (N_{60})_{av}^{0.29} \quad (11.49)$$

Correlation with Cone Penetration Test Results

In Section 11.11, the Dutch method for calculating pile tip capacity Q_p using cone penetration test results was described. In conjunction with using that method, Nottingham and Schmertmann (1975) and Schmertmann (1978) provided correlations for estimating Q_s using the frictional resistance (f_c) obtained during cone penetration tests. According to this method

$$f = \alpha' f_c \quad (11.50)$$

The variations of α' with z/D for electric cone and mechanical cone penetrometers are shown in Figures 11.20 and 11.21, respectively. We have

$$Q_s = \Sigma p(\Delta L) f = \Sigma p(\Delta L) \alpha' f_c \quad (11.51)$$

11.13

Frictional (Skin) Resistance in Clay

Estimating the frictional (or skin) resistance of piles in clay is almost as difficult a task as estimating that in sand (see Section 11.12), due to the presence of several variables that cannot easily be quantified. Several methods for obtaining the unit frictional resistance of piles are described in the literature. We examine some of them next.

λ Method

This method, proposed by Vijayvergiya and Focht (1972), is based on the assumption that the displacement of soil caused by pile driving results in a passive lateral pressure at any depth and that the average unit skin resistance is

$$f_{av} = \lambda(\bar{\sigma}'_o + 2c_u) \quad (11.52)$$

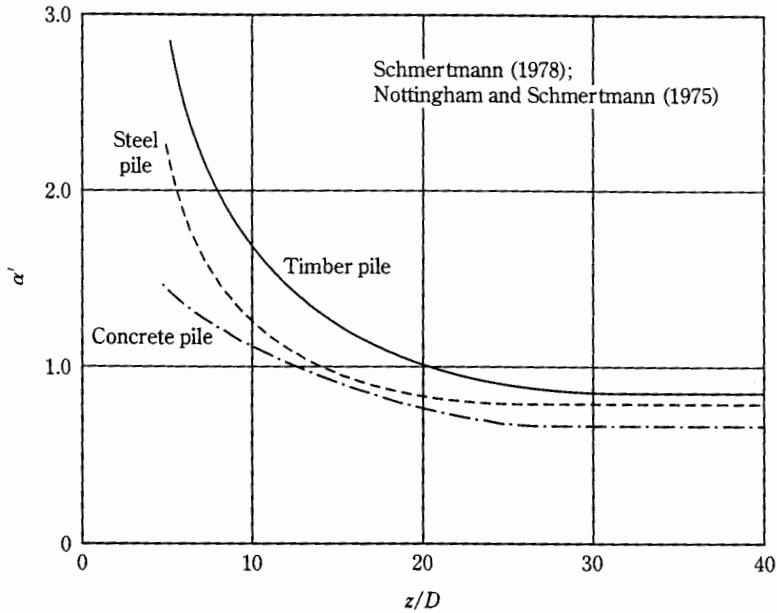


Figure 11.20 Variation of α' with embedment ratio for pile in sand: electric cone penetrometer

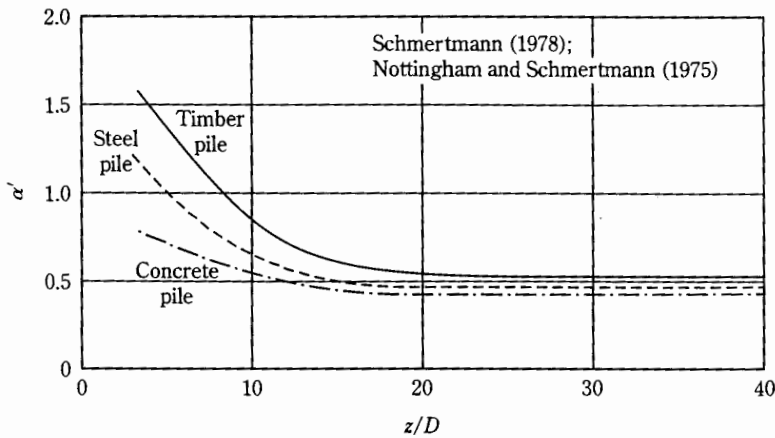


Figure 11.21 Variation of α' with embedment ratio for piles in sand: mechanical cone penetrometer

where $\bar{\sigma}'_o$ = mean effective vertical stress for the entire embedment length
 c_u = mean undrained shear strength ($\phi = 0$)

The value of λ changes with the depth of penetration of the pile. (See Figure 11.22.) Thus, the total frictional resistance may be calculated as

$$Q_s = pLf_{av}$$

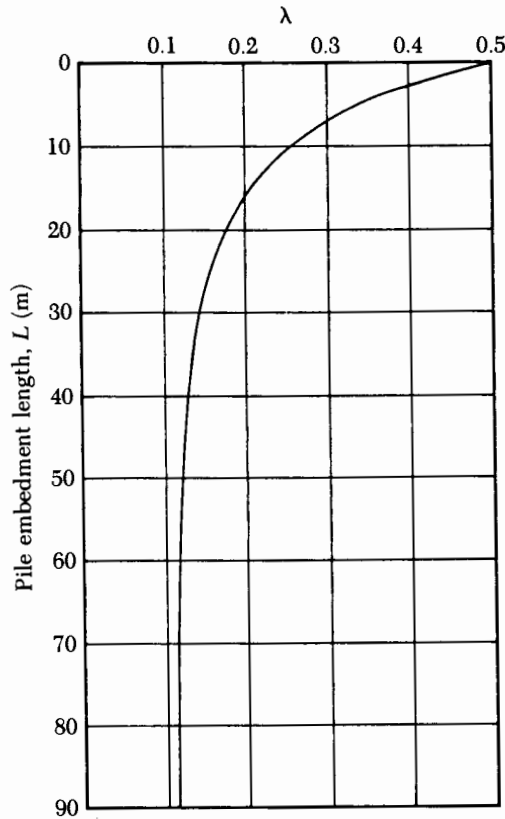


Figure 11.22 Variation of λ with pile embedment length (redrawn after McClelland, 1974)

Care should be taken in obtaining the values of $\bar{\sigma}'_o$ and c_u in layered soil. Figure 11.23 helps explain the reason. Figure 11.23a shows a pile penetrating three layers of clay. According to Figure 11.23b, the mean value of c_u is $(c_{u(1)}L_1 + c_{u(2)}L_2 + \dots)/L$. Similarly, Figure 11.23c shows the plot of the variation of effective stress with depth. The mean effective stress is

$$\bar{\sigma}'_o = \frac{A_1 + A_2 + A_3 + \dots}{L} \quad (11.53)$$

where A_1, A_2, A_3, \dots = areas of the vertical effective stress diagrams

α Method

According to the α method, the unit skin resistance in clayey soils can be represented by the equation

$$f = \alpha c_u \quad (11.54)$$

where α = empirical adhesion factor

The approximate variation of the value of α is shown in Figure 11.24,

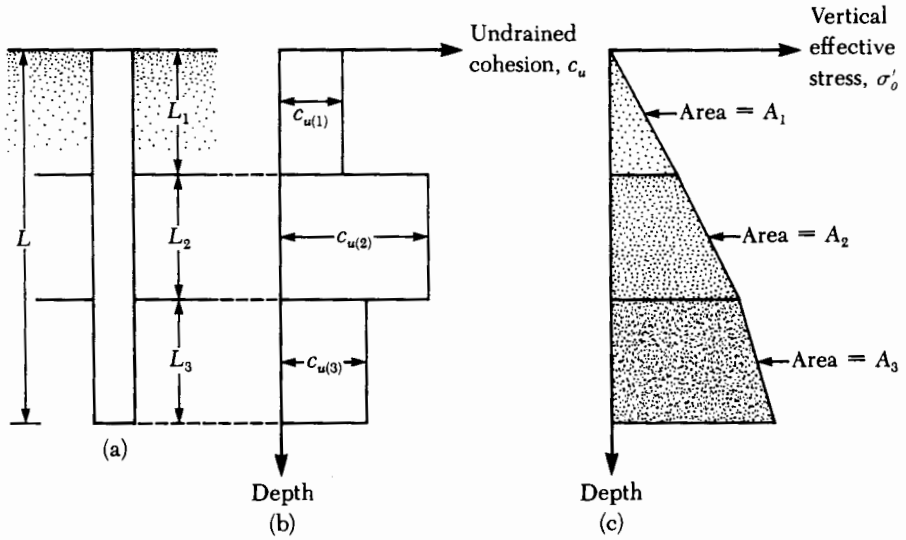


Figure 11.23 Application of λ method in layered soil

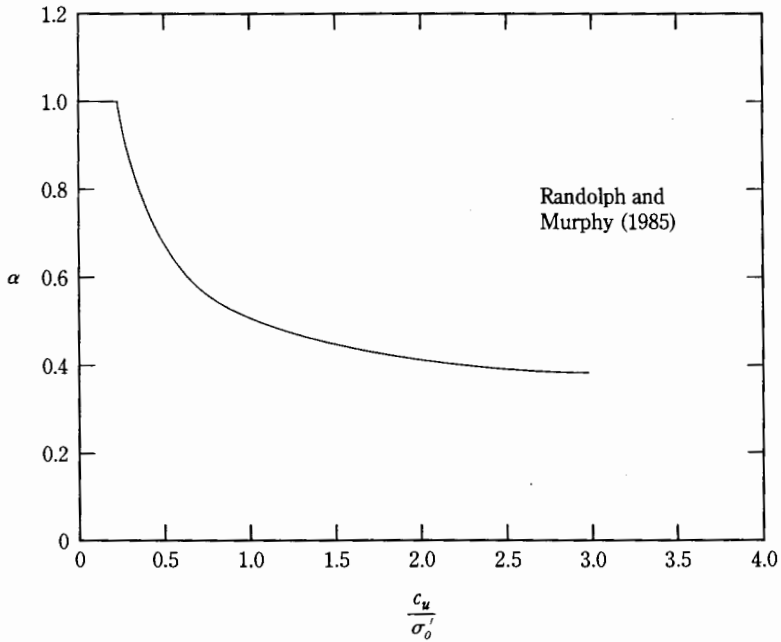


Figure 11.24 Variation of α with c_u/σ'_o

where σ'_o is the vertical effective stress. This variation of α with c_u/σ'_o was obtained by Randolph and Murphy (1985). With it, we have

$$Q_s = \sum f p \Delta L = \sum \alpha c_u p \Delta L \quad (11.55)$$

β Method

When piles are driven into saturated clays, the pore water pressure in the soil around the piles increases. The excess pore water pressure in normally consolidated clays may be four to six times c_u . However, within a month or so, this pressure gradually dissipates. Hence, the unit frictional resistance for the pile can be determined on the basis of the effective stress parameters of the clay in a remolded state ($c' = 0$). Thus, at any depth,

$$f = \beta \sigma'_o \quad (11.56)$$

where σ'_o = vertical effective stress

$$\beta = K \tan \phi'_R \quad (11.57)$$

ϕ'_R = drained friction angle of remolded clay

K = earth pressure coefficient

Conservatively, the magnitude of K is the earth pressure coefficient at rest, or

$$K = 1 - \sin \phi'_R \quad (\text{for normally consolidated clays}) \quad (11.58)$$

and

$$K = (1 - \sin \phi'_R) \sqrt{\text{OCR}} \quad (\text{for overconsolidated clays}) \quad (11.59)$$

where OCR = overconsolidation ratio

Combining Eqs. (11.56), (11.57), (11.58), and (11.59), for normally consolidated clays yields

$$f = (1 - \sin \phi'_R) \tan \phi'_R \sigma'_o \quad (11.60)$$

and for overconsolidated clays,

$$f = (1 - \sin \phi'_R) \tan \phi'_R \sqrt{\text{OCR}} \sigma'_o \quad (11.61)$$

With the value of f determined, the total frictional resistance may be evaluated as

$$Q_s = \Sigma f p \Delta L$$

Correlation with Cone Penetration Test Results

Nottingham and Schmertmann (1975) and Schmertmann (1978) found the correlation for unit skin friction in clay (with $\phi = 0$) to be

$$f = \alpha' f_c \quad (11.62)$$

The variation of α' with the frictional resistance f_c is shown in Figure 11.25. Thus,

$$Q_s = \Sigma f p (\Delta L) = \Sigma \alpha' f_c p (\Delta L) \quad (11.63)$$

11.14 General Comments and Allowable Pile Capacity

Although calculations for estimating the ultimate load-bearing capacity of a pile can be made by using the relationships presented in Sections 11.6 through 11.13, an engineer needs to keep the following points in mind:

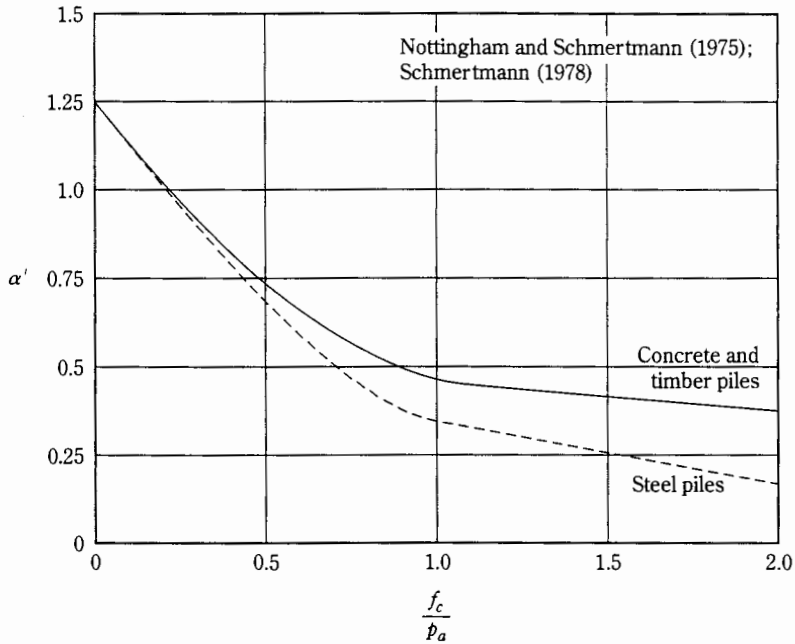


Figure 11.25 Variation of α' with f_c/p_a for piles in clay (p_a = atmospheric pressure $\approx 100 \text{ kN/m}^2$ or 2000 lb/ft^2)

1. In calculating the area of cross section, A_p , and the perimeter, p , of piles with developed profiles, such as H-piles and open-ended pipe piles, the effect of soil plug should be considered. According to Figures 11.10b and 11.10c, for pipe piles,

$$A_p = \left(\frac{\pi}{4}\right)D^2$$

and

$$p = \pi D$$

Similarly, for H-piles,

$$A_p = d_1 d_2$$

and

$$p = 2(d_1 + d_2)$$

Note that for H-piles, because $d_2 > d_1$, $D = d_1$.

2. The ultimate point load relations given in Eqs. (11.13), (11.20), and (11.30) are for the gross ultimate point load; that is, they include the weight of the pile. So the net ultimate point load is approximately

$$Q_{p(\text{net})} = Q_{p(\text{gross})} - q' A_p$$

However, in practice, for soils with $\phi' > 0$, the assumption is made that $Q_{p(\text{net})} = Q_{p(\text{gross})}$. In cohesive soils with $\phi = 0$, $N_q^* = 1$. (See Figure 11.12.) Hence, from Eq. (11.13),

$$Q_{p(\text{gross})} = (c_u N_c^* + q') A_p$$

so

$$Q_{p(\text{net})} = [(c_u N_c^* + q') - q'] A_p = c_u N_c^* A_p = 9c_u A_p = Q_p$$

This relation is the one given in Eq. (11.19).

After the total ultimate load-carrying capacity of a pile has been determined by summing the point bearing capacity and the frictional (or skin) resistance, a reasonable factor of safety should be used to obtain the total allowable load for each pile, or

$$Q_{\text{all}} = \frac{Q_u}{\text{FS}} \quad (11.64)$$

where Q_{all} = allowable load-carrying capacity for each pile
 FS = factor of safety

The factor of safety generally used ranges from 2.5 to 4, depending on the uncertainties surrounding the calculation of ultimate load.

11.15

Point Bearing Capacity of Piles Resting on Rock

Sometimes piles are driven to an underlying layer of rock. In such cases, the engineer must evaluate the bearing capacity of the rock. The ultimate unit point resistance in rock (Goodman, 1980) is approximately

$$q_p = q_u (N_\phi + 1) \quad (11.65)$$

where $N_\phi = \tan^2 (45 + \phi'/2)$
 q_u = unconfined compression strength of rock
 ϕ' = drained angle of friction

The unconfined compression strength of rock can be determined by laboratory tests on rock specimens collected during field investigation. However, extreme caution should be used in obtaining the proper value of q_u , because laboratory specimens usually are small in diameter. As the diameter of the specimen increases, the unconfined compression strength decreases—a phenomenon referred to as the *scale effect*. For specimens larger than about 1 m (3 ft) in diameter, the value of q_u remains approximately constant. There appears to be a fourfold to fivefold reduction of the magnitude of q_u in this process. The scale effect in rock is caused primarily by randomly distributed large and small fractures and also by progressive ruptures along the slip lines. Hence, we always recommend that

$$q_{u(\text{design})} = \frac{q_{u(\text{lab})}}{5} \quad (11.66)$$

Table 11.7 Typical Unconfined Compressive Strength of Rocks

Type of rock	q_u	
	MN/m ²	lb/in ²
Sandstone	70–140	10,000–20,000
Limestone	105–210	15,000–30,000
Shale	35–70	5000–10,000
Granite	140–210	20,000–30,000
Marble	60–70	8500–10,000

Table 11.8 Typical Values of Angle of Friction ϕ' of Rocks

Type of rock	Angle of friction, ϕ' (deg)
Sandstone	27–45
Limestone	30–40
Shale	10–20
Granite	40–50
Marble	25–30

Table 11.7 lists some representative values of (laboratory) unconfined compression strengths of rock. Representative values of the rock friction angle ϕ' are given in Table 11.8.

A factor of safety of at least 3 should be used to determine the allowable point bearing capacity of piles. Thus,

$$Q_{p(\text{all})} = \frac{[q_{u(\text{design})}(N_\phi + 1)]A_p}{\text{FS}} \quad (11.67)$$

Example 11.1

A concrete pile is 16 m (L) long and 410 mm \times 410 mm in cross section. The pile is fully embedded in sand for which $\gamma = 17 \text{ kN/m}^3$ and $\phi' = 30^\circ$. Calculate the ultimate point load, Q_p , by

- Meyerhof's method (Section 11.7).
- Vesic's method (Section 11.8). Use $I_r = I_{rr} = 50$.
- Janbu's method (Section 11.9). Use $\eta' = 90^\circ$.

Solution

Part a

From Eq. (11.15),

$$Q_p = A_p q' N_q^* = A_p \gamma L N_q^*$$

For $\phi' = 30^\circ$, $N_q^* \approx 55$ (see Figure 11.12), so

$$Q_p = (0.41 \times 0.41 \text{ m}^2)(16 \times 17)(55) = 2515 \text{ kN}$$

Again, from Eq. (11.17),

$$\begin{aligned} q_p &= (0.5 p_a N_q^* \tan \phi') A_p \\ &= [(0.5)(100)(55) \tan 30](0.41 \times 0.41) = 267 \text{ kN} \end{aligned}$$

Hence,

$$Q_p = 267 \text{ kN}$$

Part b

From Eqs. (11.20), (11.21), and (11.22) with $c' = 0$,

$$Q_p = A_p \sigma'_o N_\sigma^* = A_p \left[\frac{1 + 2(1 - \sin \phi')}{3} \right] q' N_\sigma^*$$

For $\phi' = 30^\circ$ and $I_{rr} = 50$, the value of N_σ^* is about 36. (See Table 11.4.) So

$$Q_p = (0.41 \times 0.41) \left[\frac{1 + 2(1 - \sin 30)}{3} \right] (16 \times 17)(36) = \mathbf{1097 \text{ kN}}$$

Part c

From Eq. (11.31) with $c' = 0$

$$Q_p = A_p q' N_q^*$$

For $\phi' = 30^\circ$ and $\eta' = 90^\circ$, the value of $N_q^* \approx 18.4$. (See Table 11.5.) Therefore,

$$Q_p = (0.41 \times 0.41)(16 \times 17)(18.4) = \mathbf{841 \text{ kN}}$$

Example 11.2

For the pile described in Example 11.1,

- Given that $K = 1.3$ and $\delta = 0.8\phi'$, determine the frictional resistance Q_s . Use Eqs. (11.14), (11.38), and (11.39).
- Using the results of Example 11.1 and Part a of this problem, estimate the allowable load-carrying capacity of the pile. Let $\text{FS} = 4$.

Solution

Part a

From Eq. (11.37),

$$L \approx 15D = 15(0.41 \text{ m}) = 6.15 \text{ m}$$

From Eq. (11.38), at $z = 0$, $\sigma'_o = 0$, so $f = 0$. Again, at $z = L' = 6.15 \text{ m}$

$$\sigma'_o = \gamma L' = (17)(6.15) = 104.55 \text{ kN/m}^2$$

So

$$f = K\sigma'_o \tan \delta = (1.3)(104.55)[\tan(0.8 \times 30)] = 60.51 \text{ kN/m}^2$$

Thus,

$$\begin{aligned} Q_s &= \left(\frac{f_{z=0} + f_{z=6.15 \text{ m}}}{2} \right) pL' + f_{6.15 \text{ m}} p(L - L') \\ &= \left(\frac{0 + 60.51}{2} \right) (4 \times 0.41)(6.15) + (60.51)(4 \times 0.41)(16 - 6.15) \\ &= 305.2 + 977.5 = \mathbf{1282.7 \text{ kN}} \end{aligned}$$

Part b

We have $Q_u = Q_p + Q_s$. From Example 11.1, the average value of Q_p is

$$\frac{267 + 1097 + 841}{3} \approx 735 \text{ kN}$$

So

$$Q_{\text{all}} = \frac{Q_u}{\text{FS}} = \frac{1}{4}(735 + 1282.7) = 504.4 \text{ kN} \quad \blacksquare$$

Example 11.3

For the pile described in Example 11.1, estimate Q_{all} using Coyle and Castello's method. [See Section 11.10 and Eq. (11.43).]

Solution

From Eqs. (11.33) and (11.43),

$$Q_u = Q_p + Q_s = q' N_q^* A_p + K \bar{\sigma}'_o \tan(0.8\phi') pL$$

and

$$\frac{L}{D} = \frac{16}{0.41} = 39$$

For $\phi' = 30^\circ$ and $L/D = 39$, $N_q^* = 25$ (see Figure 11.14) and $K \approx 0.2$ (see Figure 11.19). Thus,

$$\begin{aligned} Q_u &= (17 \times 16)(25)(0.41 \times 0.41) \\ &+ (0.2) \left(\frac{17 \times 16}{2} \right) \tan(0.8 \times 30) (4 \times 0.41)(16) \\ &= 1143 + 317.8 = 1460.8 \text{ kN} \end{aligned}$$

and

$$Q_{\text{all}} = \frac{Q_u}{\text{FS}} = \frac{1460.8}{4} = 365.2 \text{ kN} \quad \blacksquare$$

Example 11.4

A driven pipe pile in clay is shown in Figure 11.26a. The pipe has an outside diameter of 406 mm and a wall thickness of 6.35 mm.

- a. Calculate the net point bearing capacity. Use Eq. (11.19).

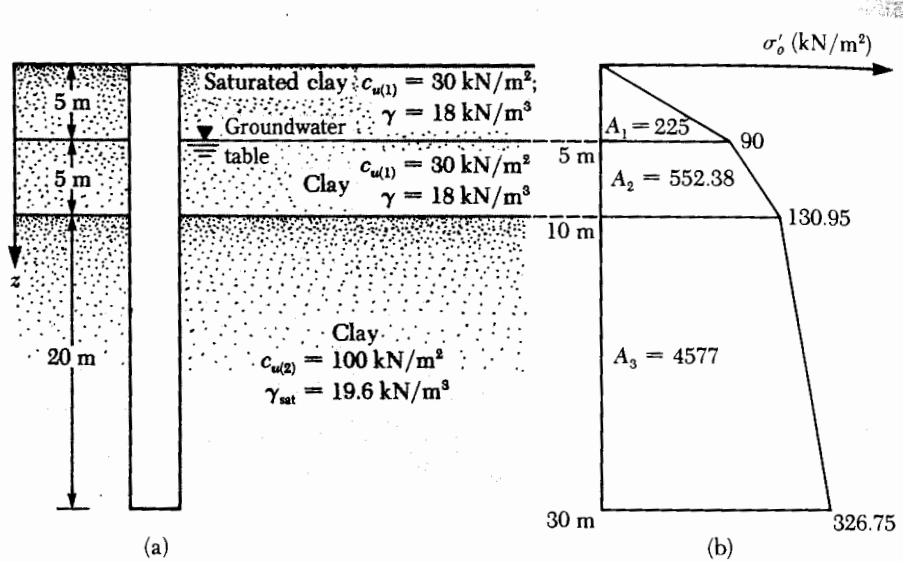


Figure 11.26 Estimation of the load bearing capacity of a driven pipe pile

- b. Calculate the skin resistance (1) by using Eqs. (11.54) and (11.55) (α method), (2) by using Eq. (11.52) (λ method), and (3) by using Eq. (11.56) (β method). For all clay layers, $\phi'_R = 30^\circ$. The top 10 m of clay is normally consolidated. The bottom clay layer has an OCR of 2.
- c. Estimate the net allowable pile capacity. Use FS = 4.

Solution

The area of cross section of the pile, including the soil inside the pile, is

$$A_p = \frac{\pi}{4} D^2 = \frac{\pi}{4} (0.406)^2 = 0.1295 \text{ m}^2$$

Part a: Calculation of Net Point Bearing Capacity

From Eq. (11.19),

$$Q_p = A_p q_p = A_p N_c^* c_{u(2)} = (0.1295) (9) (100) = \mathbf{116.55 \text{ kN}}$$

Part b: Calculation of Skin Resistance

(1) Using Eqs. (11.54) and (11.55), we have

$$Q_s = \sum \alpha c_u p \Delta L$$

The variation of vertical effective stress with depth is shown in Figure 11.26b. Now the following table can be prepared:

Depth (m)	Average depth (m)	Average vertical effective stress, $\bar{\sigma}'_o$ (kN/m ²)	c_u (kN/m ²)	$\frac{c_u}{\bar{\sigma}'_o}$ (kN/m ²)	α (Figure 11.24)
0-5	2.5	$\frac{0 + 90}{2} = 45$	30	0.67	0.6
5-10	7.5	$\frac{90 + 130.95}{2} = 110.5$	30	0.27	0.9
10-30	20	$\frac{130.95 + 326.75}{2} = 228.85$	100	0.44	0.725

Thus,

$$\begin{aligned}
 Q_s &= [\alpha_1 c_{u(1)} L_1 + \alpha_2 c_{u(1)} L_2 + \alpha_3 c_{u(2)} L_3] p \\
 &= [(0.6)(30)(5) + (0.9)(30)(5) \\
 &\quad + (0.725)(100)(20)](\pi \times 0.406) = \mathbf{2136 \text{ kN}}
 \end{aligned}$$

(2) From Eq. 11.52, $f_{av} = \lambda(\bar{\sigma}'_o + 2c_u)$. Now, the average value of c_u is

$$\frac{c_{u(1)}(10) + c_{u(2)}(20)}{30} = \frac{(30)(10) + (100)(20)}{30} = 76.7 \text{ kN/m}^2$$

To obtain the average value of $\bar{\sigma}'_o$, the diagram for vertical effective stress variation with depth is plotted in Figure 11.26b. From Eq. (11.53),

$$\bar{\sigma}'_o = \frac{A_1 + A_2 + A_3}{L} = \frac{225 + 552.38 + 4577}{30} = 178.48 \text{ kN/m}^2$$

From Figure 11.22, the magnitude of λ is 0.14. So

$$f_{av} = 0.14[178.48 + (2)(76.7)] = 46.46 \text{ kN/m}^2$$

Hence,

$$Q_s = p L f_{av} = \pi(0.406)(30)(46.46) = \mathbf{1778 \text{ kN}}$$

(3) The top layer of clay (10 m) is normally consolidated, and $\phi'_R = 30^\circ$. For $z = 0-5$ m, from Eq. (11.60), we have

$$\begin{aligned}
 f_{av(1)} &= (1 - \sin \phi'_R) \tan \phi'_R \bar{\sigma}'_o \\
 &= (1 - \sin 30^\circ)(\tan 30^\circ) \left(\frac{0 + 90}{2} \right) = 13.0 \text{ kN/m}^2
 \end{aligned}$$

Similarly, for $z = 5-10$ m.

$$f_{av(2)} = (1 - \sin 30^\circ)(\tan 30^\circ) \left(\frac{90 + 130.95}{2} \right) = 31.9 \text{ kN/m}^2$$

For $z = 10\text{--}30$ m from Eq. (11.61),

$$f_{av} = (1 - \sin \phi_R) \tan \phi_R \sqrt{\text{OCR}} \bar{\sigma}'_o$$

For OCR = 2,

$$f_{av(3)} = (1 - \sin 30^\circ) (\tan 30^\circ) \sqrt{2} \left(\frac{130.95 + 326.75}{2} \right) = 93.43 \text{ kN/m}^2$$

So

$$\begin{aligned} Q_s &= p[f_{av(1)}(5) + f_{av(2)}(5) + f_{av(3)}(20)] \\ &= (\pi)(0.406)[(13)(5) + (31.9)(5) + (93.43)(20)] = 2670 \text{ kN} \end{aligned}$$

Part c: Calculation of Net Ultimate Capacity, Q_u

We have

$$Q_{s(\text{average})} = \frac{2136 + 1778 + 2670}{3} \approx 2195 \text{ kN}$$

Thus,

$$Q_u = Q_p + Q_s = 116.55 + 2195 = 2311.55 \text{ kN}$$

and

$$3Q_{\text{all}} = \frac{Q_u}{F_s} = \frac{2311.55}{4} \approx 578 \text{ kN}$$

Example 11.5

A concrete pile 305 mm \times 305 mm in cross section is driven to a depth of 20 m below the ground surface in a saturated clay soil. A summary of the variation of frictional resistance f_c obtained from a cone penetration test is as follows:

Depth (m)	Friction resistance, f_c (kg/cm ²)
0–6	0.35
6–12	0.56
12–20	0.72

Estimate the frictional resistance Q_s for the pile.

Solution

We can prepare the following table:

Depth (m)	f_c (kN/m ²)	α' (Figure 11.25)	ΔL (m)	$\alpha' f_c p(\Delta L)$ [Eq. (11.63)] (kN)
0-6	34.34	0.84	6	211.5
6-12	54.94	0.71	6	285.5
12-20	70.63	0.63	8	434.2

Note: $p = (4)(0.305) = 1.22 \text{ m}$

Thus,

$$Q_s = \sum \alpha' f_c p(\Delta L) = 931 \text{ kN}$$

Example 11.6

An H-pile (size HP 310 × 125) having a length of embedment of 26 m is driven through a soft clay layer to rest on sandstone. The sandstone has a laboratory unconfined compression strength of 76 MN/m² and a friction angle of 28°. Use a factor of safety of 5, and estimate the allowable point bearing capacity.

Solution

From Eqs. (11.66) and (11.67),

$$Q_{p(\text{all})} = \frac{\left\{ \left[\frac{q_{u(\text{lab})}}{5} \right] \left[\tan^2 \left(45 + \frac{\phi'}{2} \right) + 1 \right] \right\} A_p}{\text{FS}}$$

From Table 11.1a, for HP 310 × 125 piles, $A_p = 15.9 \times 10^{-3} \text{ m}^2$, so

$$\begin{aligned} Q_{p(\text{all})} &= \frac{\left\{ \left[\frac{76 \times 10^3 \text{ kN/m}^2}{5} \right] \left[\tan^2 \left(45 + \frac{28}{2} \right) + 1 \right] \right\} (15.9 \times 10^{-3} \text{ m}^2)}{5} \\ &= 182 \text{ kN} \end{aligned}$$

11.16

Pile Load Tests

In most large projects, a specific number of load tests must be conducted on piles. The primary reason is the unreliability of prediction methods. The vertical and lateral load-bearing capacity of a pile can be tested in the field. Figure 11.27a shows a schematic diagram of the pile load arrangement for testing *axial compression* in the field. The load is applied to the pile by a hydraulic jack. Step loads are applied to the pile, and